



Cite this: *Mater. Adv.*, 2021, 2, 6996

Received 7th August 2021,  
Accepted 22nd September 2021

DOI: 10.1039/d1ma00700a

rsc.li/materials-advances

## Fabrication of polypyrrole/Cu(II) nanocomposite through liquid/liquid interfacial polymerization: a novel catalyst for synthesis of NH-1,2,3-triazoles in PEG-400†

Parmita Phukan,<sup>‡a</sup> Rupkamal Chetia,<sup>‡a</sup> Ratan Boruah,<sup>b</sup> Surajit Konwer<sup>ID</sup>\*<sup>a</sup> and Diganta Sarma<sup>ID</sup>\*<sup>a</sup>

In the present paper, we have reported the synthesis and application of a polypyrrole (PPy)/Cu(II) nanocomposite as an efficient heterogeneous catalyst for the synthesis of 4-aryl-NH-1,2,3-triazoles. The nanocomposite was prepared via liquid/liquid interfacial polymerization where copper and initiator (FeCl<sub>3</sub>) were dispersed in the aqueous phase and the monomer was dissolved in the organic phase. The synthesized sample was characterized by Fourier transform infrared spectroscopy (FTIR), scanning electron microscopy (SEM), energy dispersive X-ray spectroscopy (EDX), X-ray diffraction (XRD), transmission electron microscopy (TEM) and inductively coupled plasma atomic emission spectroscopy (ICP-AES). Spectroscopic analyses showed the successful incorporation of Cu in the polymer matrix and the decoration of copper nanoparticles within the PPy matrix was observed from the morphological analysis. Herein, we have developed a simple one-pot, multi-component system using a PPy/Cu catalyst for the synthesis of NH-triazoles. Keeping in view the principles of green chemistry, the reactions were performed in the low-cost and environmentally friendly solvent polyethylene glycol 400 (PEG 400). A very low loading of copper (0.01 mol%) catalyzed the reaction very efficiently with an excellent yield of the desired product. Furthermore, the catalytic system can be recovered and recycled up to 5th subsequent cycle, maintaining its catalytic activity with excellent yields of triazoles. To the best of our knowledge no previous work has been reported for the synthesis of 4-aryl-NH-1,2,3-triazoles using this efficient novel catalyst.

## Introduction

Pi-conjugated polymer nanocomposites have become an attractive area in nanoscience due to their diverse applications in

various fields, such as super capacitors,<sup>1</sup> battery electrodes,<sup>2</sup> sensors,<sup>3</sup> catalysts<sup>4</sup> and many other fields.<sup>5</sup> The addition of a small quantity of nanofiller can dramatically improve various properties of the polymer nanocomposite due to which they have attracted a lot of attention in recent research fields.<sup>6</sup> Out of many conducting polymers, polypyrrole (PPy) is one of the most important conducting polymers due to its good redox behavior, electrical conductivity, ease of preparation and good environmental stability.<sup>7</sup> The exceptional physical properties and electrochemical behavior of PPy with pronounced stability towards air make it more interesting in the field of research.<sup>8</sup> The presence of a pi-conjugated polymer within the catalyst system not only acts as a binder but also improves the activity of the catalyst. PPy possesses high conductivity due to the positive charge created on its backbone. During polymerization, the polypyrrole matrix balances its electrical neutrality by incorporating anions from solution. In our work, FeCl<sub>3</sub> is used as the oxidizing agent and it provides a Cl<sup>−</sup> ion as a counter ion. PPy is unique because it can switch its state from a conducting (oxidized form) to an insulating state (reduced or neutral form) (Scheme 1).

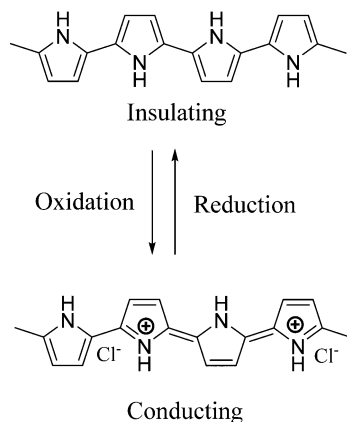
1,2,3-Triazoles are a very fundamental class of N-heterocycles that are indispensable motifs in many biologically essential compounds, such as anti-cancer, anti-HIV, anti-bacterial, anti-microbial and anti-allergic drug molecules.<sup>9–13</sup> Due to their unique properties, such as high chemical stability, strong dipole moment, aromatic character *etc.*, this class of heterocyclic moieties is extensively used in drug discovery, material chemistry, and bio-pharmaceutical and medicinal chemistry.<sup>14,15</sup> Moreover, 1,2,3-triazoles are of significant importance as photo-stabilizers, dyes, agrochemicals and corrosion inhibitors.<sup>16,17</sup> Among 1,2,3-triazole compounds, 4-aryl-NH-1,2,3-triazoles have gained tremendous interest in the field of the pharmaceutical industry.<sup>18–21</sup> Research reveals that many medicinally relevant scaffolds are composed of amide bonds. Interestingly, the close similarity of NH-triazoles to amide bonds has been successfully utilized in the synthesis of a large

<sup>a</sup> Department of Chemistry, Dibrugarh University, Dibrugarh-786004, Assam, India.  
E-mail: dsarma22@gmail.com, surajitkonwer@dibru.ac.in; Tel: +9854403297

<sup>b</sup> Department of Physics, Tezpur University, Tezpur-784028, Assam, India

† Electronic supplementary information (ESI) available: Analytical data of the synthesized compounds including copies of <sup>1</sup>H and <sup>13</sup>C NMR spectra are included in the supporting information. See DOI: 10.1039/d1ma00700a

‡ These authors contributed equally to this article.



Scheme 1 Conducting and insulating forms of polypyrrole.

number of privileged drug molecules (Fig. 1).<sup>22</sup> The literature reveals that NH-triazole molecules act as a unique template for the inhibition of human methionine amino peptidase (hMetAP2) inhibitors and indoleamine 2,3-dioxygenase (IDO).<sup>23,24</sup> NH-triazoles also serve as important precursors for the arylation of 1,2,3-triazoles<sup>25</sup> as well as key intermediates for a series of fundamental organic transformations.<sup>26</sup> Due to the versatile and significant importance of 4-aryl-NH-1,2,3-triazoles, it is of utmost importance to develop efficient and suitable methodologies to access this structural motif.

Over the past few decades, there has been significant awareness pertaining to the strict legislation on the maintenance of the “principles of green chemistry” in all synthetic applications and pathways.<sup>27,28</sup> Hence, in order to eliminate the use of hazardous organic solvents from chemical industries, an important goal of current research is to introduce non-toxic, cost-effective and non-volatile “green solvents”.<sup>29–32</sup> In recent years, PEGs have served as a suitable alternative to conventional organic solvents due to their attractive physico-chemical properties, such as thermal stability, chemical inertness,

non-toxicity and their being mostly non-immunogenic. PEGs are stable even at high temperature *i.e.* up to 150–200 °C and show good solubility both in water and in many organic solvents. In organic syntheses some of the eminent applications of this class of green solvent include Williamson ether synthesis, oxidation and reduction reactions, and coupling reactions.<sup>33,34</sup> These superior properties offer PEG as the new gold standard as a green alternative solvent in the current scientific and research arena. Current research in synthetic chemistry has observed the renaissance of multicomponent reactions (MCRs) as a powerful tool for the synthesis of complex organic molecules *via* operational simplicity and easy purification of the product. MCRs allow the formation of multiple bonds in a single step and hence render several advantages, such as convergence, facile automation, extraction and purification processes, *etc.* In addition, MCRs minimize the reaction time, thereby increasing the overall yield of product formation. In 1838, Laurent and Gerhardt first reported multicomponent reactions.<sup>35</sup> Since then, many research groups have incorporated MCRs in synthetic reactions, such as Ugi,<sup>36</sup> Biginelli,<sup>37</sup> Hantzsch,<sup>38</sup> and Strecker,<sup>39</sup> including the efficient synthesis of 1,2,3-triazoles.<sup>40</sup>

While designing a new catalyst, the key points are its easy separation from the products and the possibility of recycling. In this respect, nanosized metallic catalysts in solid supports create a prospective type of catalytic material. The formation of nano-catalysts in the redox-polymerization of a heterocyclic precursor oxidized by metal ions is a promising approach for catalytic application.<sup>41</sup> When Cu is encapsulated in PPy, the polymer matrix provides a large surface area for easy dispersion of the Cu metal. Additionally, the redox behaviour of polypyrrole seems to provide a convenient support for the active phase of the oxidative-reductive catalyst. This synergistic effect and the redox properties of polypyrrole with Cu particles are believed to enhance the catalytic activity of the catalyst towards the efficient synthesis of NH-1,2,3-triazoles.

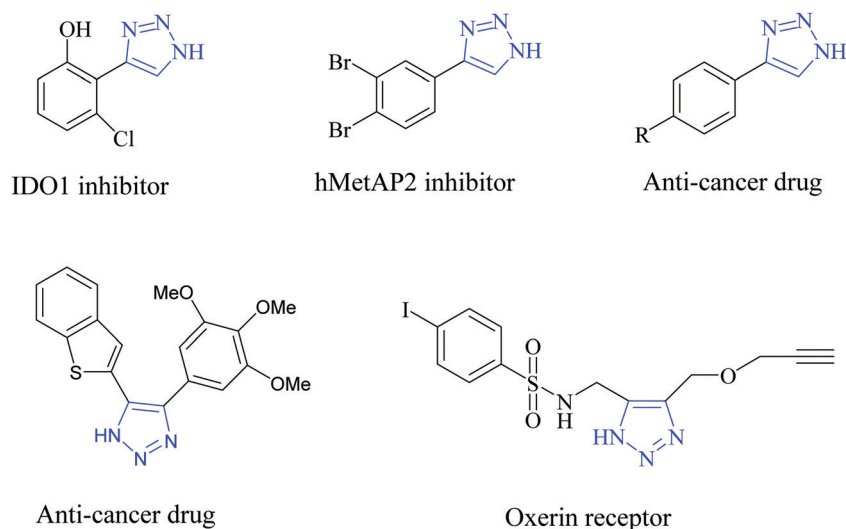


Fig. 1 Biologically active NH-1,2,3-triazoles.



Based on the above findings and observations, we are hereby reporting for the first time the use of a copper(II) filled polypyrrole nanocomposite as a heterogeneous catalyst for the synthesis of 4-aryl-NH-1,2,3-triazoles. To the best of our knowledge, no study has been conducted on the combined PPy and copper(II) nanocomposite for triazole preparation.

## Experimental

### Materials

Pyrrole monomer was purchased from Spectrochem Pvt. Limited, Mumbai, India. Ferric chloride (anhydrous) was obtained from Alpha Chemical. Copper(II) sulfate pentahydrate was procured from Merck. Carbon tetrachloride was obtained from Paskem Fine Chemical. PEG-400 (Merck), Nitromethane ( $\text{CH}_3\text{NO}_2$ , 98%, TCI), nitroethane ( $\text{C}_2\text{H}_5\text{NO}_2$ , 98%, Spectrochem), sodium azide ( $\text{NaN}_3$ , 99%, Spectrochem) and all aldehydes (Spectrochem with 98% purity) were purchased and used without any further purification. The products obtained were purified by column chromatography over silica gel (120–200 mesh). Thin-layer chromatography was carried out using silica gel 60F<sub>254</sub> plates and visualized under UV light.

### Preparation of polypyrrole/Cu(II) nanocomposite

A liquid/liquid interfacial polymerization method was used to prepare the polypyrrole/copper nanocomposite (Scheme 2). Initially, 3 mL of pyrrole monomer was dissolved in 17 mL of carbon tetrachloride in a beaker to obtain the organic phase. 10 mL of 0.01 M aq. copper sulfate solution and 10 mL of 0.05 M aq. ferric chloride solution (which acts as an initiator) was mixed together to form the aqueous phase. Subsequently, the aqueous phase was added to the organic phase dropwise. The beaker was then kept undisturbed for the next 24 hours. Throughout this time, it was observed that a thin black film developed slowly in the interface between the organic and aqueous phases. The product thus obtained was filtered and washed several times with deionised water and ethanol to remove impurities, unused  $\text{FeCl}_3$  and any other soluble organic byproducts. Eventually the product was air dried and used as a catalyst for NH-1,2,3-triazole synthesis (Scheme 3).

### General procedure for the synthesis of NH triazoles

A mixture of aromatic aldehyde (1 mmol), nitroalkane (2 mmol), sodium azide (3 mmol) and polypyrrole/copper (PPy-Cu) catalyst (5 mg) was stirred at 100 °C in 2 mL of PEG-400 solvent under aerobic conditions. The reaction progress was monitored

by TLC. After completion, the reaction mixture was allowed to cool at room temperature and extracted by ethyl acetate (3 × 10 mL). The organic layer was then dried over anhydrous sodium sulfate followed by concentrating the filtrate under reduced pressure. The final product obtained was then purified by column chromatography over silica gel by using a mixture of ethyl acetate/hexane. The purified products were characterized by  $^1\text{H}$  and  $^{13}\text{C}$  NMR spectroscopy (ESI<sup>†</sup>).

## Results and discussion

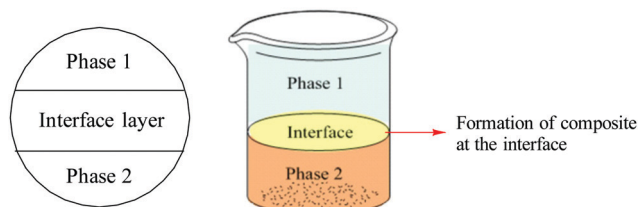
### Characterization of the as-synthesized catalyst

The morphology of the newly synthesized catalyst was characterized by transmission electron microscopy (TEM), as shown in Fig. 2.<sup>42</sup> The images demonstrate that the PPy/Cu(II) nanocomposite has a spherical morphology and the composite exhibits discrete spheres with an average diameter in the range of ~20 nm to ~80 nm. This may be due to the active surface entrapment of the polymer and stabilization of the Cu by immobilizing and preventing their aggregation into larger particles.<sup>43</sup>

SEM micrographs of the PPy and the PPy/Cu catalyst are depicted in Fig. 3(a and b), respectively. The SEM image of pristine polymer indicates the hemispherical nature of the polymer. Interestingly, the SEM image of the as-synthesized catalyst was found to be quite similar, but the particles are bigger in size compared to the pristine polymer, which may be due to the good distribution of copper metal in the polymer backbone. This uniform distribution of copper over the polymer surface escalated their catalytic activity, resulting in satisfactory yields of the desired product.

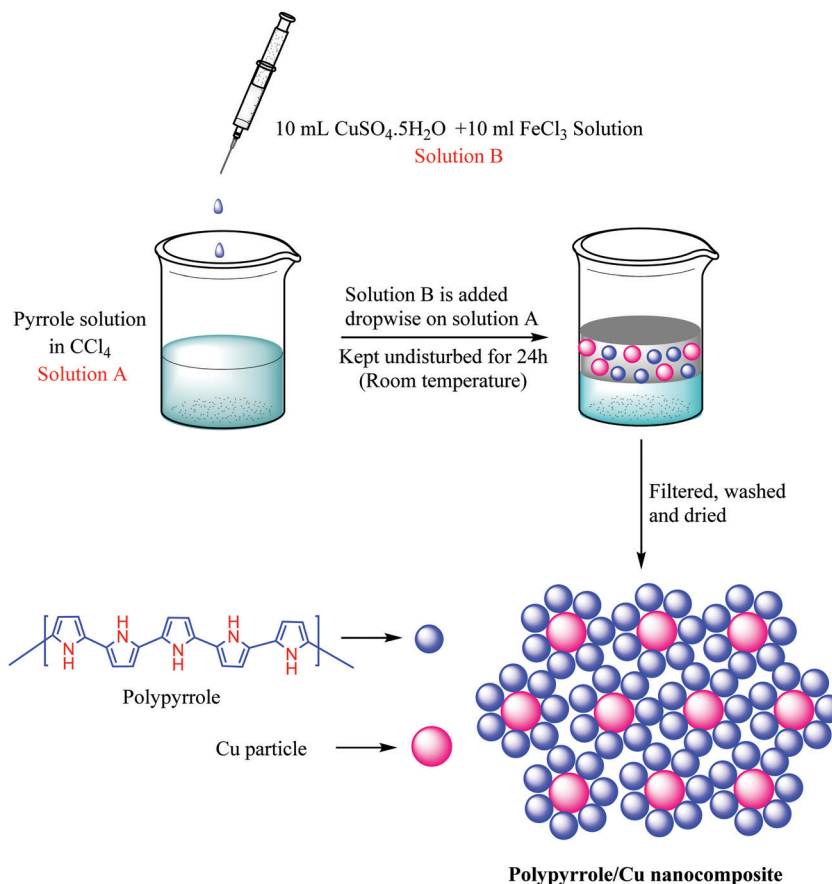
The compositional analysis of the synthesized catalyst was further analyzed by an energy dispersive X-ray (EDX) spectroscopy study (Fig. 4). The EDX spectrum of the PPy/Cu(II) catalyst showed various peaks of copper, carbon and nitrogen, which confirmed the presence of these elements in the composite structure. The copper peak was mainly due to the copper source; carbon and nitrogen peaks came from the polymer unit. The peak for oxygen can be attributed to the open air reaction conditions employed during the preparation of the catalyst. The peak around 2.6 in the EDX spectrum corresponds to the  $\text{Cl}^-$  ion, present in the nanocomposite. When  $\text{FeCl}_3$  attacks the monomers, the monomers get converted into positively charged species by donating electrons to  $\text{Fe}^{3+}$  and the  $\text{Cl}^-$  ion binds with these positive charges to maintain the electrical neutrality of the polymer. The  $\text{Cl}^-$  ions which are not utilized as counter ions are washed off with water. Due to the  $\text{Cl}^-$  ions present in the nanocomposite which act as counter ions, a peak arises at around 2.6 in the EDX spectrum of the nanocomposite.

The X-ray diffraction pattern (XRD) depicts the successful incorporation of the copper metal into the matrix of the polymer. The XRD pattern of pure PPy and PPy/Cu composite are represented in Fig. 5(a and b), respectively. The intense diffraction peak at a  $2\theta$  value of  $26.65^\circ$  is the characteristic peak



Scheme 2 Pictorial representation of interfacial polymerization.





**Scheme 3** Schematic representation for the preparation of polypyrrole/copper nanocomposite.

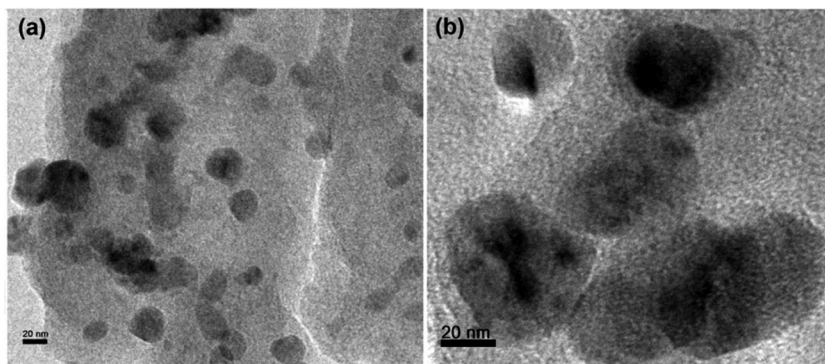


**Fig. 2** TEM images of the catalyst at (a) low magnification and (b) high magnification.

of the crystalline PPy. In the PPy/Cu composite three sharp peaks are observed. The characteristic peak at  $2\theta = 25.3^\circ$  represents PPy. The diffraction peaks at  $2\theta = 10.42^\circ$  and  $42.4^\circ$  can be attributed to the standard cubic phases of copper.<sup>44</sup>

The FTIR spectra of PPy and the PPy/Cu composite were recorded in the range of  $4000\text{ cm}^{-1}$  to  $400\text{ cm}^{-1}$ . In the FT-IR spectrum of PPy (Fig. 6), the strong bands at  $3433\text{ cm}^{-1}$ ,  $2926\text{ cm}^{-1}$  and  $1578\text{ cm}^{-1}$  correspond to the absorption of N-H stretching, C-H stretching and C=C ring stretching of

pyrrole, respectively. The bands at  $1380\text{ cm}^{-1}$ ,  $1187\text{ cm}^{-1}$  and  $1042\text{ cm}^{-1}$  are due to C-H vibration, C-C stretching and in-plane deformation of C-H bond of pyrrole ring, respectively.

The characteristic absorptions of PPy in the PPy/Cu composite can be observed in Fig. 7. The peaks at  $3097\text{ cm}^{-1}$  and  $2930\text{ cm}^{-1}$  correspond to N-H and C-H stretching and the strong bands at  $1558\text{ cm}^{-1}$  and  $1200\text{ cm}^{-1}$  represent C-C and aromatic C-H stretching vibration in the pyrrole ring, respectively. The band of C-H in-plane deformation vibration is





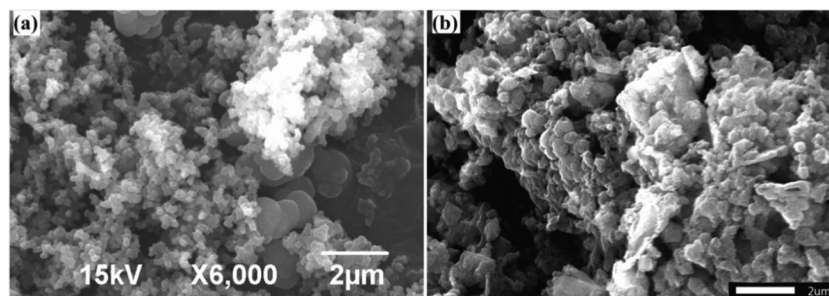


Fig. 3 SEM images of (a) pure PPy and the (b) PPy/Cu nanocomposite.

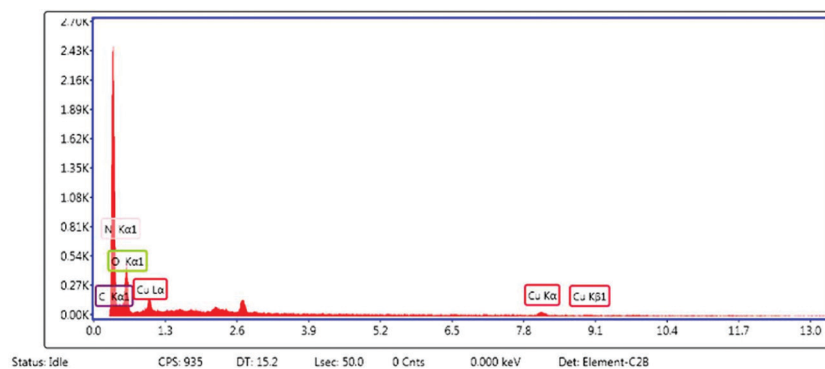


Fig. 4 EDX spectrum of the synthesized PPy/Cu(II) nanocomposite.

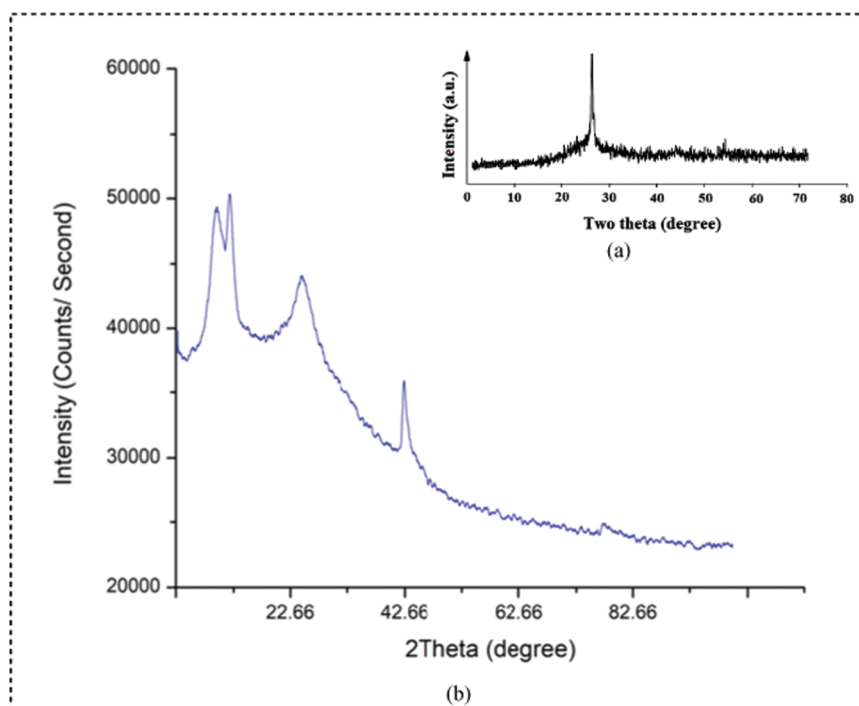


Fig. 5 XRD of (a) pure PPy and the (b) PPy/Cu nanocomposite.

situated at  $1048\text{ cm}^{-1}$  and the peak at  $921\text{ cm}^{-1}$  is due to out-of-plane ring deformation. The peak at  $777\text{ cm}^{-1}$  corresponds to

the C-H wagging vibrations. The FTIR spectral wavelength and intensity of the peaks of the PPy/Cu(II) nanocomposite showed a



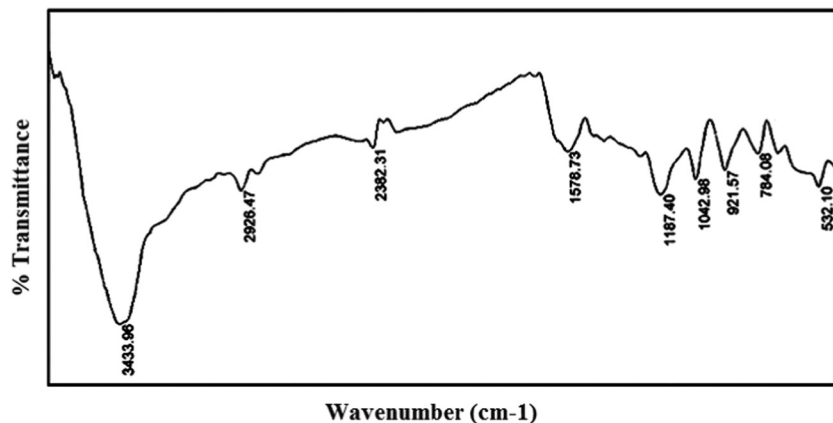


Fig. 6 FTIR of pure PPy.

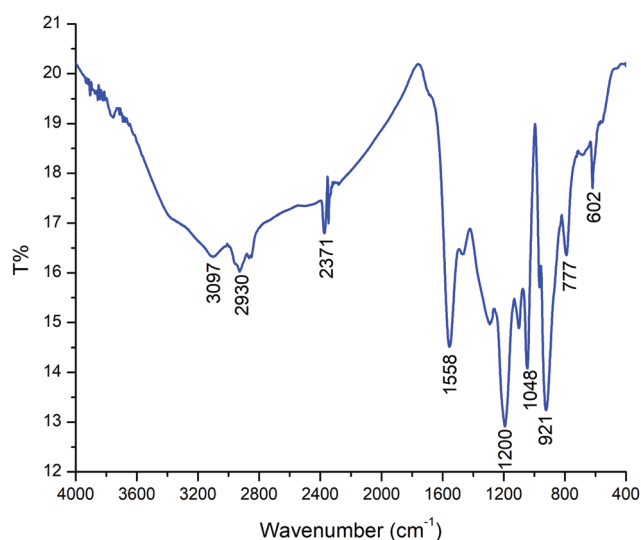


Fig. 7 FTIR spectra of the PPy/Cu(II) nanocomposite.

Table 1 Optimization of catalyst quantity in the synthesis of 4-aryl-NH-1,2,3-triazoles<sup>a</sup>

Entry	Catalyst (mg)	Time (h)	Yield <sup>b</sup> (%)
1	20	1	96
2	15	1	96
3	10	1	96
4	5	1	96
5	2	2	84
6	—	2	25
7	5	0.5	85
		0.25	68

<sup>a</sup> Reaction conditions: 4-bromobenzaldehyde (1 mmol), nitromethane (2 mmol), NaN<sub>3</sub> (3 mmol), catalyst, solvent (PEG-400) (2 mL), in air. <sup>b</sup> Isolated yield.

peak shift compared to pristine Ppy, as reported elsewhere, which indicates the incorporation of Cu(II) nanoparticles into the PPy ring.

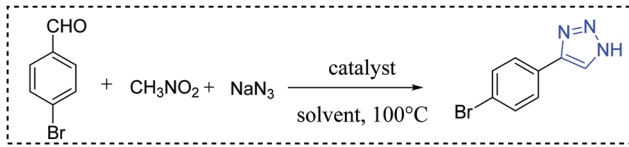
### Catalytic study

At the very outset, we investigated the catalytic performance of the as-synthesized PPy–Cu catalyst towards NH-triazole synthesis by taking 4-bromo-benzaldehyde, nitromethane and sodium azide as the model substrates under various reaction parameters. Initially, the effect of the catalytic amount of PPy–Cu catalyst that is required for the effective synthesis of NH-triazole products was explored (Table 1, entries 1–7). As can be seen from Table 1, 20 mg of the catalyst produced 96% of the desired product within just an hour (Table 1, entry 1). Decreasing the amount of catalyst to 15 mg and 10 mg also afforded the requisite product with satisfactory yield (Table 1, entries 2 and 3). The catalytic significance of the synthesized catalyst was then investigated by decreasing the catalyst loading to 5 mg affording 96% yield in 1 hour duration (Table 1, entry 4).

However, a further decrease in catalyst loading resulted in a slight decrease in the yield of the product along with longer consumption of time (Table 1, entry 5). The necessity for the catalyst in the reaction was confirmed by a controlled experiment carried out in the absence of the catalyst. The reaction in the absence of the catalyst produced NH-triazoles in poor yield (Table 1, entry 6).

Encouraged by the significant performance of the catalyst towards NH-triazole synthesis, we then extended our study to determine the suitable solvent and temperature for the efficient synthesis of NH-triazoles (Table 2, entries 1–12). Initially, the reaction was performed under neat conditions, taking 4-bromo-benzaldehyde, nitromethane and sodium azide as the model substrates at 100 °C under aerobic conditions. Notably, a poor yield of the requisite product was obtained (Table 2, entry 1). Being the universal solvent, water was used as solvent but not much improvement in reaction kinetics was observed, affording poor yield (Table 2, entry 2). As a result, a wide variety of organic solvents were investigated and moderate yields were



Table 2 Optimization of the reaction conditions<sup>a</sup>


Entry	Solvent	Temperature (°C)	Time (h)	Yield <sup>b</sup> (%)
1	—	100	1	30
2	H <sub>2</sub> O	100	1	55
3	DMSO	100	1	72
4	DMF	100	1	71
5	DCM	100	1	78
6	Toluene	100	1	49
7	EG	100	1	81
8	EG:H <sub>2</sub> O	100	1	78
9	DMSO:H <sub>2</sub> O	100	1	75
10	PEG-400	100	1	98
11	PEG-400	70	1	72
12	PEG-400	RT	24	Trace
13 <sup>c</sup>	PEG-400	100	1	35
14 <sup>d</sup>	PEG-400	100	1	30

<sup>a</sup> Reaction conditions: 4-bromobenzaldehyde (1 mmol), nitromethane (2 mmol), NaN<sub>3</sub> (3 mmol) and catalyst (5 mg), solvent (2 mL), in air. <sup>b</sup> Isolated yield. <sup>c</sup> Controlled reaction using CuSO<sub>4</sub> (0.1 mol%). <sup>d</sup> Controlled reaction using PPy (0.1 mol%).

obtained (Table 2, entries 3–9) in each case. Keeping in view the principles of green chemistry, the efficiency of the solvent PEG 400 was explored and interestingly the best results were obtained in this case (Table 2, entry 10). Additionally, optimization of the reaction temperature was also performed by lowering the temperature to 70 °C but a poor yield of the product was observed (Table 2, entry 11). As a controlled experiment the reaction was investigated at room temperature as well, but only a trace amount of the product was found (Table 2, entry 12). Moreover, the reaction was performed using CuSO<sub>4</sub> (0.1 mol%) as catalyst. It was found that, a much lower amount of product could be isolated in this case. Hence, after investigating a wide array of optimal parameters, 5 mg of PPy–Cu catalyst (0.01 mol% Cu, from ICP-AES analysis) in PEG 400 as green solvent at 100 °C were found to be the optimized conditions in our present study.

With the optimized reactions conditions in hand, the scope of the PPy–Cu catalyst was then explored towards a wide range of electronically diverse aldehydes (Scheme 4, entries a–n). As exemplified in Scheme 4, all the reactions proceeded very smoothly, affording the requisite product in excellent yield with high purity. All substrates, with *ortho*-, *meta*- or *para*-substitution showed satisfactory reactivity towards the formation of NH-triazole product. Aromatic aldehydes bearing halogen atoms, such as Br, Cl and F, afforded the requisite NH-triazole in excellent yields. Salicylaldehyde and 2,4-dichlorobenzaldehyde also proceeded very smoothly with the as-synthesized catalyst affording the desired product in satisfactory yields (Scheme 4, entries f and g). Furthermore, the heterocyclic moieties thiophen-2-aldehyde and furan-2-aldehyde also reacted efficiently, resulting in an excellent yield of NH-triazole product (Scheme 4, entries i and j). In order to

extend the scope of the synthesized catalyst, the reactivity of another nitroalkane, *i.e.* nitroethane, was investigated under optimized reaction conditions. Pleasingly, it was found that in the presence of nitroethane, the reaction also proceeded quite smoothly, affording the requisite triazole in excellent yields (Scheme 4, entries k–n).

In this work, PPy is used as a catalyst support to enhance the catalytic activity of a composite. PPy can exist in several oxidation states: in neutral, oxidized or reduced forms.<sup>45,46</sup> It can undergo protonation/deprotonation in the polymer chain and can also interact with dopants.<sup>47,48</sup> *In situ* polymerization of a pyrrole monomer leads to the formation of a polypyrrole matrix which stabilizes the Cu particles on its surface and prevents it from aggregation. As a result, there is no need to add surface stabilizers. PPy itself has no catalytic activity, but the polypyrrole matrix provides a large surface area, thereby improving the dispersion of copper in the composite material. This synergistic effect of polypyrrole with Cu particles is believed to enhance the catalytic activity of the catalyst towards the efficient synthesis of NH-1,2,3-triazoles.

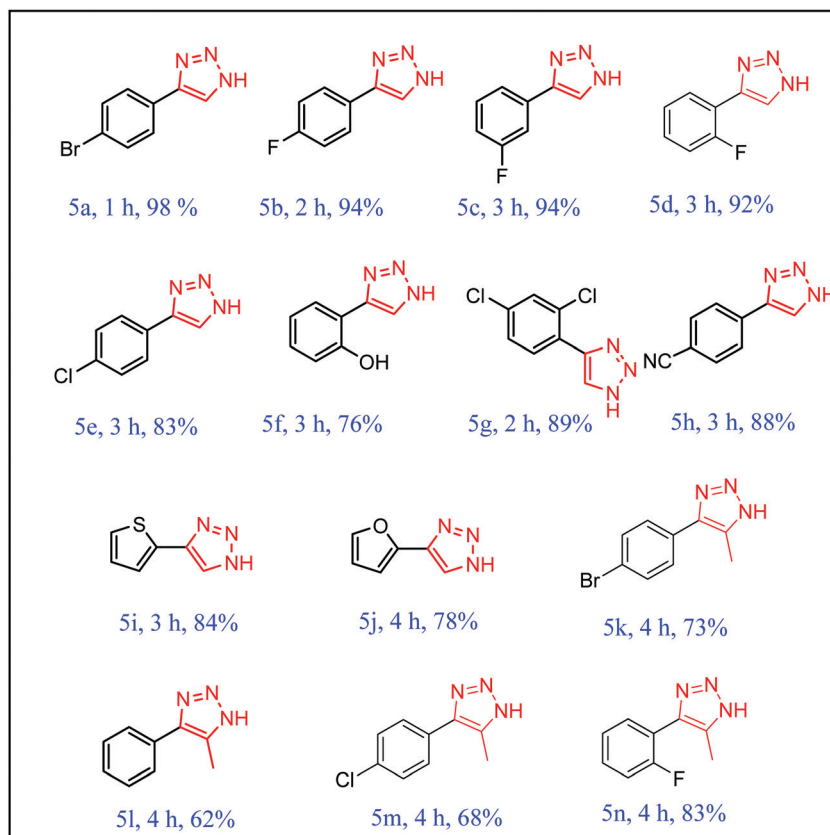
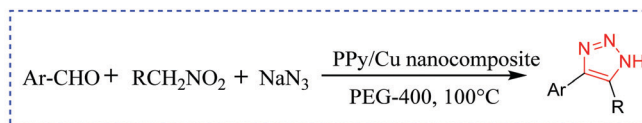
On the basis of literature reports,<sup>22,49</sup> here we have proposed a plausible mechanism for this reaction (Scheme 5). Initially, aromatic aldehyde reacts with nitromethane in the presence of sodium azide to form nitroolefin (A). The catalytic reaction proceeds *via* the coordination of nitroolefin in the surface of the PPy/Cu catalyst (B) followed by nucleophilic addition of sodium azide, leading to the formation of intermediate C. Subsequently, intermediate C undergoes cyclization followed by elimination of HNO<sub>2</sub>. In the final step, the desired 4-aryl-NH-1,2,3-triazole product is formed by utilizing a proton from the solvent (D).

Furthermore, we have tested the catalytic efficiency of our catalyst for the synthesis of two IDO1 inhibitors, namely, 4-phenyl-1H-1,2,3-triazole and 4-(2-chlorophenyl)-1H-1,2,3-triazole (Scheme 6, entries i and ii). It is worth mentioning that both reactions proceeded smoothly, resulting in a satisfactory yield of the desired IDO1 inhibitors (Scheme 6).

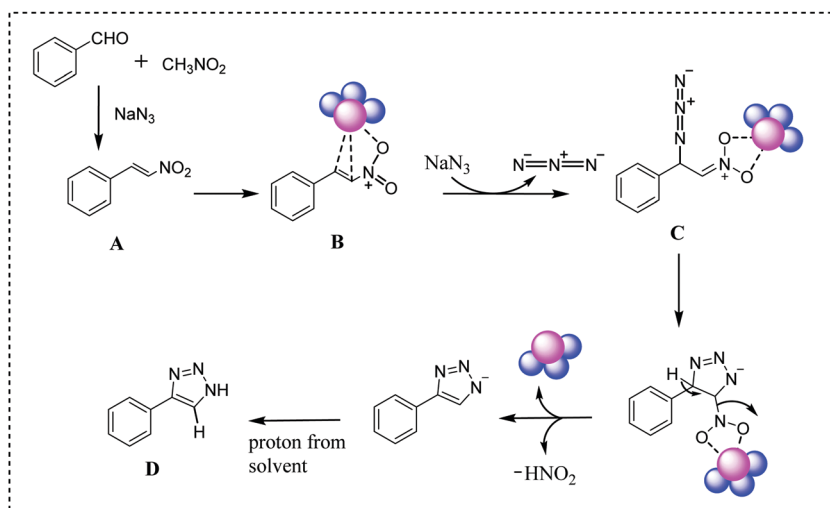
### Recyclability of the catalytic system

In order to emphasize the synthetic utility of the catalytic system, the recyclability of the catalyst as well as the solvent was investigated (Scheme 7). A consecutive one-pot, three-component reaction was carried out using 4-bromobenzaldehyde, nitromethane and sodium azide with the PPy/Cu catalyst in PEG 400 as solvent. After successful completion of the first cycle, the reaction mixture was extracted with diethyl ether (3 × 10 mL). The organic layer was then separated, leaving behind the catalyst dispersed in PEG 400 solvent. A subsequent 2nd cycle of the reaction was carried out with the catalyst along with the PEG 400 solvent with the same substrates but without the addition of extra solvent or catalyst. Interestingly, a quite consistent result was obtained in the 2nd cycle as well. The results of consecutive cycles confirmed that our catalytic medium, including both the catalyst and the solvent, can be effectively reused up to 5th cycle without notable loss in its catalytic activity. It was observed that the





Scheme 4 PPy/Cu(III) nanocomposite catalyzed NH triazole synthesis.



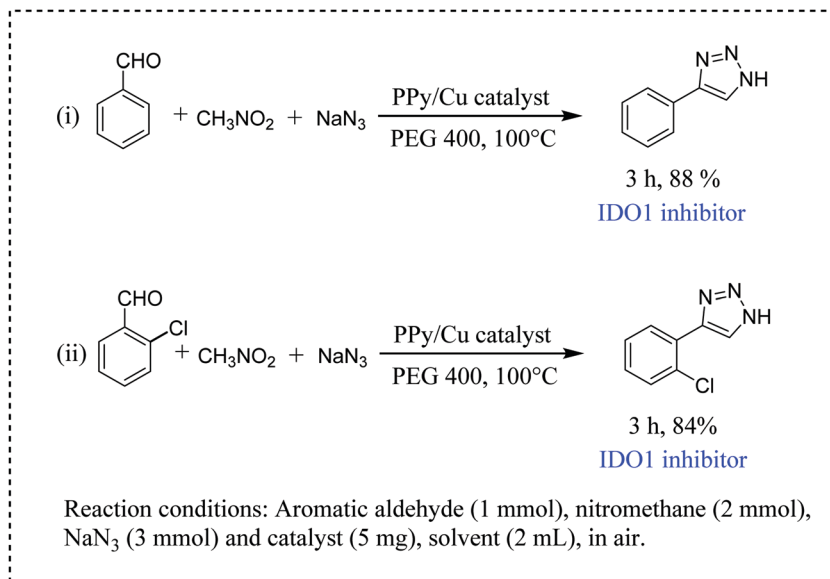
Scheme 5 Plausible mechanism for PPy/Cu nanocomposite catalysed NH-triazole synthesis.

catalytic activity of the PPy/Cu nanocomposite slightly decreased in the 5th cycle (89%) because of which we did not

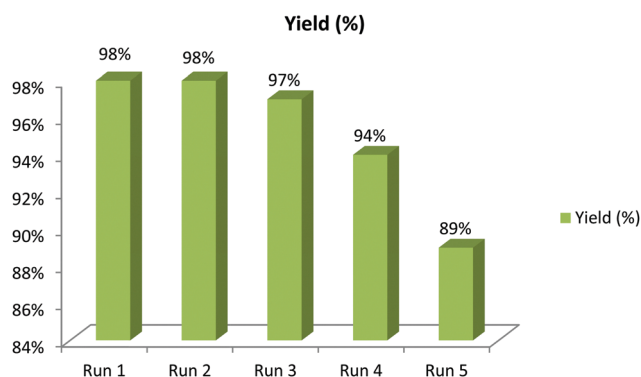
proceed to further cycles. The slight decrease in yield of the product may be due to a gradual physical loss during the







**Scheme 6** Synthesis of two pharmaceutically important NH-1,2,3-triazoles.



**Scheme 7** Reusability of the catalytic system.

process of separation, filtration and washing performed after each consecutive run.

A few literature reports are depicted in Table 3 to compare the efficiency of our synthesized catalyst with other catalytic

**Table 3** Comparison of catalytic efficiency of our PPy/Cu nanocatalyst with reported catalytic systems for the synthesis of 4-aryl-NH-1,2,3-triazoles

Entry	Catalyst	Solvent	Temperature (°C)	Yield (%)	Ref.
1	PPy/Cu nanocomposite	PEG 400	100	98	Our work
2	$\text{Fe}_3\text{O}_4$ @Folic acid	Choline azide	80	85	50
3	$\text{NH}_4\text{OAc}/\text{HOAc}$	DMF	100	79	51
4	$\text{NaHSO}_3/\text{Na}_2\text{SO}_3$	DMSO	110	71	52

methods. To our delight, the catalytic efficiency of the newly synthesized catalyst was found to be quite satisfactory, resulting in excellent yields of the desired products.

## Conclusion

We have designed a significant polypyrrole/copper(II) nanocomposite *via* liquid/liquid interfacial polymerization. The morphology along with the structural analysis of the catalyst was investigated by several characterization techniques, such as TEM, SEM, EDX, XRD, IR and ICP-AES analysis. The as-synthesized catalyst acted as an efficient catalyst for the synthesis of a wide variety of 4-aryl-NH-triazoles with extremely low copper loading (0.01 mol%). Moreover, the catalyst along with the solvent PEG 400 can be recovered easily and reused up to 4th consecutive cycle, maintaining the consistency of the catalytic activity. According to a literature analysis, this catalytic system represents a novel approach towards the synthesis of 4-aryl-NH-1,2,3-triazoles with several advantages, such as high reactivity, operational simplicity and easy recyclability.

## Running head

NH-1,2,3-triazole synthesis in green solvent.

## Data availability statement

The data that supports the findings of this study are available in the ESI† of this article.

## Conflicts of interest

The authors declare no competing financial interest.



## Acknowledgements

The authors thank Dibrugarh University for providing all the infrastructural facility, Tezpur University for TEM, SEM, XRD and FTIR analysis. We acknowledge Department of Science and Technology for financial assistance under the DST-FIST programme and UGC, New Delhi for Special Assistance Programme (UGC-SAP) to the Department of Chemistry, Dibrugarh University.

## References

- 1 S. Konwer, R. Boruah and S. K. Dolui, *J. Electron. Mater.*, 2011, **40**, 2248–2255.
- 2 J. Wang, J. Chen, K. Konstantinov, L. Zhao, S. H. Ng, G. X. Wang, Z. P. Guo and H. K. Liu, *Electrochim. Acta*, 2006, **51**, 4634–4638.
- 3 S. Konwer, A. K. Guha and S. K. Dolui, *J. Electron. Mater.*, 2013, **48**, 1729–1739.
- 4 H. Zhao, L. Li, J. Yang, Y. Zhang and H. Li, *Electrochem. Commun.*, 2008, **10**, 876–879.
- 5 H. D. da Rocha, E. S. Reis, G. P. Ratkovski, R. J. da Silva, F. D. Gorza, G. C. Pedro and C. P. de Melo, *J. Taiwan Inst. Chem. Eng.*, 2020, **110**, 8–20.
- 6 C. K. Madhusudhan, K. Mahendra, B. S. Madhukar, T. E. Somesh and M. Faisal, *Synth. Met.*, 2020, **267**, 116450.
- 7 P. Camurlu, *RSC Adv.*, 2014, **4**, 55832–55845.
- 8 M. Joulazadeh and A. H. Navarchian, *Synth. Met.*, 2015, **210**, 404–411.
- 9 N. Pribut, C. G. Veale, A. E. Basson, W. A. Van Otterlo and S. C. Pelly, *Bioorg. Med. Chem. Lett.*, 2016, **26**, 3700–3704.
- 10 H. M. Savanur, K. N. Naik, S. M. Ganapathi, K. M. Kim and R. G. Kalkhambkar, *ChemistrySelect*, 2018, **3**, 5296–5303.
- 11 P. V. Chavan, U. V. Desai, P. P. Wadgaonkar, S. R. Tapase, K. M. Kodam, A. Choudhari and D. Sarkar, *Bioorg. Chem.*, 2019, **85**, 475–486.
- 12 A. A. Abd-Rabou, B. F. Abdel-Wahab and M. S. Bekheit, *Chem. Pap.*, 2018, **72**, 2225–2237.
- 13 K. Lal and P. Yadav, *Anti-Cancer Agents Med. Chem.*, 2018, **18**, 21–37.
- 14 M. A. Tasdelen and Y. Yagci, *Angew. Chem., Int. Ed.*, 2013, **52**, 5930–5938.
- 15 C. Gill, G. Jadhav, M. Shaikh, R. Kale, A. Ghawalkar, D. Nagargoje and M. Shiradkar, *Bioorg. Med. Chem. Lett.*, 2008, **18**, 6244–6247.
- 16 P. Thirumurugan, D. Matosiuk and K. Jozwiak, *Chem. Rev.*, 2013, **113**, 4905–4979.
- 17 Y. H. Lau, P. J. Rutledge, M. Watkinson and M. H. Todd, *Chem. Soc. Rev.*, 2011, **40**, 2848–2866.
- 18 Q. Hu, Y. Liu, X. Deng, Y. Li and Y. Chen, *Adv. Synth. Catal.*, 2016, **358**, 1689–1693.
- 19 U. F. Röhrig, S. R. Majjigapu, A. Grosdidier, S. Bron, V. Stroobant, L. Pilotte, D. Colau, P. Vogel, B. J. Van den Eynde, V. Zoete and O. Michielin, *J. Med. Chem.*, 2012, **55**, 5270–5290.
- 20 Q. Huang, M. Zheng, S. Yang, C. Kuang, C. Yu and Q. Yang, *Eur. J. Med. Chem.*, 2011, **46**, 5680–5687.
- 21 P. Phukan, S. Agarwal, K. Deori and D. Sarma, *Catal. Lett.*, 2020, **150**, 2208–2219.
- 22 A. Garg, D. Sarma and A. A. Ali, *Curr. Res. Green Sustain. Chem.*, 2020, **3**, 100013.
- 23 T. Weide, S. A. Saldanha, D. Minond, T. P. Spicer, J. R. Fotsing, M. Spaargaren, J. M. Frère, C. Bebrone, K. B. Sharpless, P. S. Hodder and V. V. Fokin, *ACS Med. Chem. Lett.*, 2010, **1**, 150–154.
- 24 L. S. Kallander, Q. Lu, W. Chen, T. Tomaszek, G. Yang, D. Tew, T. D. Meek, G. A. Hofmann, C. K. Schulz-Pritchard, W. W. Smith and C. A. Janson, *J. Med. Chem.*, 2005, **48**, 5644–5647.
- 25 U. F. RoHrig, L. Awad, A. Grosdidier, P. Larrieu, V. Stroobant, D. Colau, V. Cerundolo, A. J. G. Simpson, P. Vogel, B. J. Van den Eynde and V. Zoete, *J. Med. Chem.*, 2010, **53**, 1172–1189.
- 26 S. Ueda, M. Su and S. L. Buchwald, *Angew. Chem.*, 2011, **123**, 9106–9109.
- 27 H. A. Swarup, K. Mantelingu and K. S. Rangappa, *ChemistrySelect*, 2018, **3**, 703–708.
- 28 R. A. Sheldon, *Chem. Soc. Rev.*, 2012, **41**, 1437–1451.
- 29 P. Tundo, P. Anastas, D. S. Black, J. Breen, T. J. Collins, S. Memoli, J. Miyamoto, M. Polyakoff and W. Tumas, *Pure Appl. Chem.*, 2000, **72**, 1207–1228.
- 30 D. J. C. Constable, C. J. Gonzalez and R. K. Henderson, *Org. Process Res. Dev.*, 2007, **11**, 133–137.
- 31 F. M. Perna, P. Vitale and V. Capriati, *Curr. Opin. Green Sustain. Chem.*, 2020, **21**, 27–33.
- 32 M. Cvjetko Bubalo, S. Vidović, I. Radojčić Redovniković and S. Jokić, *J. Chem. Technol. Biotechnol.*, 2015, **90**, 1631–1639.
- 33 Y. Gu and F. Jérôme, *Green Chem.*, 2010, **12**, 1127–1138.
- 34 G. Jin, C. Zhang, T. Ido and S. Goto, *Catal. Lett.*, 2004, **98**, 107–111.
- 35 A. Laurent and C. F. Gerhardt, *Ann. Chim. Phys.*, 1838, **66**, 181.
- 36 I. Ugi, R. Meyr, U. Fetzer and C. Steinbrückner, *Angew. Chem.*, 1959, **71**, 386.
- 37 P. Biginelli, *Chem. Ber.*, 1891, **24**, 1317–1319.
- 38 A. Hantzsch, *Chem. Ber.*, 1881, **14**, 1637–1638.
- 39 A. Strecker, *Ann. Chem. Pharm.*, 1854, **91**, 349–351.
- 40 A. Garg, A. A. Ali, K. Damarla, A. Kumar and D. Sarma, *Tetrahedron Lett.*, 2018, **59**, 4031–4035.
- 41 T. V. Magdesieva, O. M. Nikitin, O. A. Levitsky, V. A. Zinovyeva, I. Bezverkhyy, E. V. Zolotukhina and M. A. Vorotyntsev, *J. Mol. Catal. A: Chem.*, 2012, **353**, 50–57.
- 42 J. Liu, M. Li, W. G. Li, Y. K. Liu and J. S. Yao, *Adv. Mater. Res.*, 2012, **557**, 254–257.
- 43 R. Ansari, *Eur. J. Chem.*, 2006, **3**, 186–201.
- 44 J. Marimuthu and M. Rajasekhar, *IOSR J. Appl. Chem.*, 2017, **10**, 51–55.
- 45 V. W. L. Lim, E. T. Kang and K. G. Neoh, *Synth. Met.*, 2001, **123**, 107–115.
- 46 M. T. Galkowski, P. J. Kulesza, K. Miecznikowski, M. Chojak and H. Bala, *J. Solid State Electrochem.*, 2004, **8**, 430–434.



- 47 M. Hasik, A. Bernasik, A. Adamczyk, G. Malata, K. Kowalski and J. Camra, *Eur. Polym. J.*, 2003, **39**, 1669–1678.
- 48 S. Sadki, P. Schottland, N. Brodiec and G. Sabouraud, *Chem. Soc. Rev.*, 2000, **29**, 283–293.
- 49 S. Payra, A. Saha and S. Banerjee, *ChemCatChem*, 2018, **10**, 5468–5474.
- 50 S. Bagheri, M. J. Nejad, F. Pazoki, M. K. Miraki and A. Heydari, *ChemistrySelect*, 2019, **4**, 11930–11935.
- 51 R. Hui, M. Zhao, M. Chen, Z. Ren and Z. Guan, *Chin. J. Chem.*, 2017, **35**, 1808–1812.
- 52 L. Wu, X. Wang, Y. Chen, Q. Huang, Q. Lin and M. Wu, *Synlett*, 2016, 437–441.

